

## Bachelorarbeit

# Fracturing of model cohesive granulates

# Rissbildung in kohäsiven Modellgranulaten

angefertigt von

**Alexander Heinrich Schmeink**

aus Tübingen

am Max Planck Institut für Dynamik und Selbstorganisation

**Bearbeitungszeit:** 1. November 2013 bis 28. Januar 2014

**Betreuer/in:** Markus Benderoth

**Erstgutachter/in:** Dr. Lucas Goehring

**Zweitgutachter/in:** Prof. Dr. Eberhard Bodenschatz



# Contents

<b>1. Introduction</b>	<b>1</b>
<b>2. Materials and Methods</b>	<b>3</b>
2.1. The model cohesive granulate . . . . .	3
2.1.1. Glass beads . . . . .	4
2.1.2. PDMS . . . . .	5
2.1.3. Mixture . . . . .	5
2.1.4. Preparation of a sediment sample . . . . .	5
2.2. Bacteria . . . . .	6
2.3. Elasticity . . . . .	7
<b>3. Experimental setup</b>	<b>9</b>
3.1. Qualitative properties of the sample . . . . .	9
3.2. Structure reconstruction - Xray-tomography . . . . .	10
3.3. Elasticity measurement - The scale setup . . . . .	11
3.4. Microscopy . . . . .	12
<b>4. Analysis</b>	<b>13</b>
4.1. Qualitative properties of the sample . . . . .	13
4.2. Structure reconstruction . . . . .	14
4.3. Scale setup . . . . .	15
4.3.1. Stress and strain calculation . . . . .	15
4.3.2. Visualisation of data . . . . .	16
4.3.3. Behavior in deformation . . . . .	17
4.3.4. Curing time . . . . .	19
4.3.5. PDMS content . . . . .	21
4.3.6. PDMS composition . . . . .	22
4.4. Microscopy . . . . .	23

*Contents*

<b>5. Discussion</b>	<b>27</b>
5.1. Qualitative properties of the granulate . . . . .	27
5.2. Structure reconstruction . . . . .	27
5.3. Scale . . . . .	28
5.4. Microscopy . . . . .	28
<b>6. Concluding remarks</b>	<b>31</b>
<b>A. Appendix</b>	<b>33</b>

# 1. Introduction

When water is added to sand, the result is a material which can be sculpted to obtain a solid shape. This material property of wet granular matter in general (not only sand) is due to capillary forces, which result from the surface tension of the liquid and make the material stiff and cohesive [1][2]. The properties of granular matter and wet granular matter have been in the focus of researchers for the last four decades, presenting amazing results. For example, the Brazil nut effect refers to the fact that when a granulate of different sized particles is being shaken the larger grains tend to raise to the surface [1]. Another surprising fact about granular matter is that next to being a solid it can behave like a liquid or a gas as can be observed in an hour glass or sand storms. This includes the possibility of phase changes.

Although theoretical research can go far, experimental evidence is needed to support the findings and inspire new questions to ask. For experiments with cemented granulates there is still a lack of working models. A working model should be easy to use and highly controllable in its properties, for example tensile strength and elasticity. It is the goal of this thesis to establish a packing of glass beads with a polymer forming elastic bridges as a working model for experiments on cohesive granular matter.

This thesis is part of a project, which will use this new working model for research on the topic of biodeterioration. Biodeterioration is defined by Hueck as “any undesirable change in the properties of a material caused by the vital activities of micro-organisms“[3][4]. Biodeterioration occurs in stone buildings and is a combination of physical, chemical, and biological degradation processes, enhancing each other [5]. An example for a biochemical component of biodeterioration is degradation through the metabolism of micro-organisms in a direct (assimilation) or indirect (dissimilation) way [3]. The fracturing of our cohesive granulate will be the experimental model for a biophysical component of biodeterioration, namely the cracking of a porous stone through the pressure induced by the cell growth of micro-organisms.



## 2. Materials and Methods

In this chapter we introduce the model cohesive granulate and its ingredients, give a small introduction to our model of elasticity used to describe the granulate, and give basic information on the bacteria we are planning to use for the fracturing.

### 2.1. The model cohesive granulate

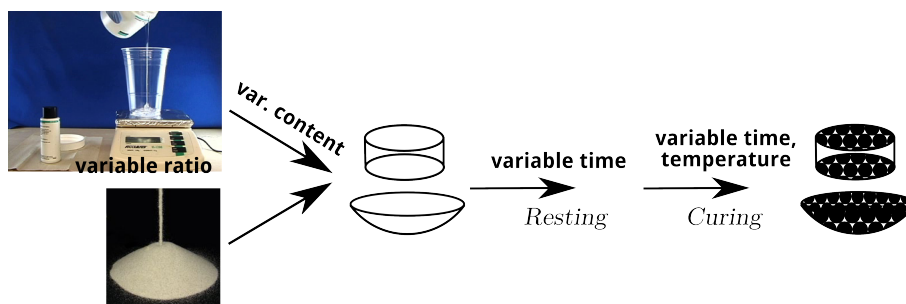


Figure 2.1.: Workflow of the experiment. The samples consist of glass beads and PDMS, moulded into a cylindrical or lenticular shape. Resting time ensures homogeneous spreading of the the liquid PDMS across the sample. Curing secures the bridges, making them solid and elastic. After the samples are cured, they can be used in the different experiments we conducted. The variable parameters are base - curing agent ration, PDMS volume fraction, resting time, curing time, and curing temperature. The images are taken from [6],[7]

In the experiment we use a packing of glass beads which are connected by elastic bridges of the polymer PDMS (polydimethylsiloxane). **Image 2.1** shows how the ingredients become a sample to be used in the experiments. The fact that the glass beads are sticking together makes the packing a cohesive granulate. When cured, the PDMS keeps the packing in a rigid, but elastic structure. We call this model cohesive granulate 'sediment sample' or just 'sample'. The quality of a sediment sample is

## 2. Materials and Methods

determined by its homogeneity and pore space<sup>1</sup>. Homogeneity ensures comparable results when measuring different samples. The size of pores is important, because we plan to grow microorganisms in samples of the same type, which need to be supplied with nutrients. To yield samples with a high pore space we choose to prepare samples in the *pendular regime*. It is characterised by capillary bridges connecting two beads each. In the pendular regime the pore space consists of one pore system spreading through the entire sample. Likewise, all solid matter is connected. **Image A.1** (see appendix) shows different regimes of wetness in a sample [1].

### 2.1.1. Glass beads

Since glass beads show the same chemical behavior as sand, they are used in several model systems [2] for experiments on wet granular matter. We use spherical glass beads with diameters between 150 and 250  $\mu\text{m}$ . The material has a density of  $\rho_{\text{material}} = 2.5 \frac{\text{g}}{\text{cm}^3}$ . A quick check, where a known mass of glass beads is poured into a measuring cylinder filled with water, confirms this value.

However, the effective density<sup>2</sup> of loosely packed glass beads is smaller, since there is always air between the beads. To find out the effective density we measure the mass of sand which fills the inside volume of a cylinder completely. The inside volume of the cylinder is  $V_{\text{tube}} = 47.7 \text{cm}^3$  (height: 120mm, diameter: 22.5mm). We find that a mass  $m = (68.7 \pm 0.5) \text{g}$  of sand fills the volume of the cylinder completely. This means that only a volume of

$$\frac{m}{\rho_{\text{sand}}} = (27.5 \pm 0.2) \text{cm}^3$$

is accounted for by the sand. This corresponds to a fraction of  $(57.6 \pm 0.5) \text{vol}\%$  of sand inside the tube. The rest of the volume is pores filled by air. As the density of air has units of  $1.0 \cdot 10^{-3} \frac{\text{g}}{\text{cm}^3}$ , it is negligible in this calculation. So the effective density of the glass sand inside the tube is

$$\rho_{\text{eff}} := \frac{m}{V_{\text{tube}}} = 1.44 \pm 0.01 \frac{\text{g}}{\text{cm}^3}. \quad (2.1)$$

---

<sup>1</sup>Volume which is not occupied by beads or bridge material.

<sup>2</sup>The ratio of total mass and total volume of a packing of glass beads.



### 2.1.2. PDMS

The polymer we use for cementing the granulate is Polydimethylsiloxane (PDMS) of the type Sylgard 184, which is originally liquid, but becomes a solid when cured. PDMS consists of the polymer-containing base and a crosslinking-agent at a ratio of for example 10:1. The fraction of crosslinking-agent has an impact on the stiffness or elasticity of cured PDMS. For example, PDMS in a base-agent ratio of 5:1 is stiffer than of 10:1. In the bulk, PDMS cures within a day at room temperature or in one hour at 75°C. Inside the sediment sample, liquid PDMS comes in capillary bridges, which have a tiny volume and a huge contact area with solid beads. As a result, in the experiment PDMS cures differently than in the bulk. We want to find out after what time capillary bridges of PDMS cure to become solid bridges of capillary shape. In the bulk, PDMS of the usual ratio (10:1) has a density of  $\rho_{PDMS} = 1.1 \frac{\text{g}}{\text{cm}^3}$  [8][9], a kinematic viscosity of  $\nu_{PDMS} = 0.5 \frac{\text{m}}{\text{s}^2}$  when uncured and a YOUNG's modulus in the order of  $10^6$  Pa.

### 2.1.3. Mixture

As mentioned before, a high pore space of connected pores is crucial to supply micro-organisms inside the sample with nutrients from the outside. Therefore we chose to prepare our samples in the pendular regime to ensure that all pores are connected. In the pendular regime, the total volume of capillary bridges lies between 0.5 and 3% of the packing's total volume[1]. In addition to the pore space we have to care for the sample's stability. A too small PDMS content will cause soft and instable samples we cannot use in experiments with micro-organisms.

### 2.1.4. Preparation of a sediment sample

Preparing a sample requires several steps, starting with the preparation of the ingredients and ending with the curing of the sample. The glass beads which are used have to be cleaned with different solvents from dust, salts, grease, and pieces of carbon black, which are relics of the heating during glass production. We do this by rinsing a portion of sand with ethanol (for grease), then isopropanol (for microorganisms) and at last water (for dust and carbon black) until the alcohols are gone. The clean and dried beads are then used for the preparation of sediments. Polymer-base and curing-agent are mixed in a mass ratio of for example 10:1 to produce liquid PDMS. This is done in a disposable plastic cup using a plastic fork

## 2. Materials and Methods

to stir the mixture. During stirring, bubbles form in the PDMS. Before combining it with the glass beads we use a vacuum pump to pull the bubbles to the surface of the PDMS and let it rest for ten minutes in the vacuum until the bubbles are gone. We always aim for a desired volume fraction  $c \in \mathfrak{R}^{[1;3]}$  of polymer in the sample. The right amount of PDMS for a given mass of beads is determined by this formula, which uses the density of PDMS and the effective density of packed glass beads (see **equation 2.1**):

$$\frac{m_{beads}}{\rho_{eff}} \cdot \frac{c}{1-c} \cdot \rho_{PDMS} = m_{PDMS} \quad (2.2)$$

To make sure the PDMS is spread homogeneously in the glass beads, we stir for three minutes. The result is a paste of wetted glass beads.

In the next step the paste is moulded into a plexiglas-tube. By compressing the paste in the mould, we make sure there are no rifts or cracks inside the sample to begin with. Afterwards the sample has to rest for 2 hours. This gives the PDMS time to form nice capillary bridges between the beads. In the last step the PDMS has to cure to secure the bridges. This is done in an oven at either 50°C or 75°C. To be sure the PDMS would be cured, we worked with curing times around 15 hours. For the experiments we varied the parameters base-curing agent mass ratio, PDMS volume fraction, resting time, curing time, and curing temperature (see **image 2.1**).

## 2.2. Bacteria

The bacteria used in the experiment are of the type *escherichia coli*. E. coli is a bacterium  $1\mu\text{m}^3$  in size living in the large intestine of mammals [10]. It is widely studied, easily obtainable, not very sensitive to its environment, and not dangerous for humans. It is also easy to feed with a high growth rate. Therefore it is easy and inexpensive to use for experiments. E. coli is rated as *facultative anaerobic*, which means that it is capable of *aerobic respiration*<sup>3</sup> as well as *fermentation*<sup>4</sup> when there is no oxygen about.

---

<sup>3</sup>Glucose + Oxygen  $\rightarrow$  CO<sub>2</sub> + Water + Heat

<sup>4</sup>Glucose  $\rightarrow$  Ethanol + CO<sub>2</sub>

## 2.3. Elasticity

The elasticity of a material can be described by the YOUNG's modulus  $E$ , which is in the linear case defined as the ratio of stress  $\sigma$  and strain  $\varepsilon$ :

$$E = \frac{\sigma}{\varepsilon} \Leftrightarrow \sigma = E \cdot \varepsilon \quad (2.3)$$

$\sigma$  is the pressure on a body and has units [Pa], while  $\varepsilon$  is the deformation of a body, divided by its initial length and is therefore dimensionless. As the sediment sample is not a solid block, but made of spherical beads, the stress is distributed to the elastic bridges between the individual beads. This suggests a nonlinear elastic model to describe our sample. The simplest of such models is that of elasticity of 3rd order in energy, developed by LANDAU [11][12]. In its general form and in absence of shear a quadratic term is added to the linear stress term:

$$\sigma = E \cdot \varepsilon + C \cdot \varepsilon^2 \quad (2.4)$$

$C$  is one of three general LANDAU moduli with units [Pa]. We will see that the third order elasticity model sufficiently describes our samples.



## 3. Experimental setup

We want to find out which are key parameters to ensure homogeneity inside the sample and how to control its elasticity. The focus on elasticity is due to the project's goal to let micro-organisms crack samples. Not only do we need to be able to make the samples soft enough for the organisms to crack. For measuring the force exerted by the organisms to cause a crack, we need to know the elasticity of the sample which was cracked. In this chapter we introduce four experiments we used to examine samples and single out the key parameters in sample building.

### 3.1. Qualitative properties of the sample

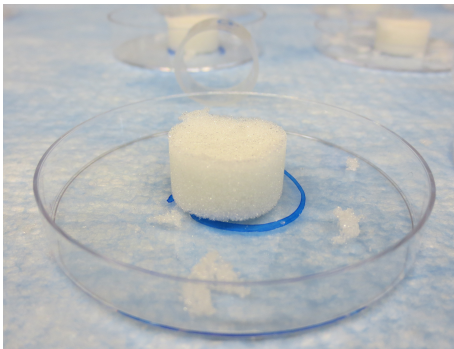


Figure 3.1.: Sample with small plexiglas ring. The diameter of the sample is  $d = 18.20 \pm 0.05$  mm.

In qualitative properties experiment examination of the samples is done by hand and eye, as we want to get an idea of the basic dependencies between for example the amount of PDMS in a sample and its qualitative properties (elasticity, cohesion, homogeneity). We use small rings of plexiglas (inner diameter  $d = 18.20 \pm 0.05$  mm, height  $\approx 10$  mm) as moulds for our samples as shown in **Image 3.1**. The samples are cured over night at either  $50^\circ\text{C}$  or  $75^\circ\text{C}$ . We also vary the PDMS volume fraction in the samples from 1-3 vol%. Furthermore we use a microwave oven to heat up some of the samples before putting them in the normal oven. The idea is to heat

the samples more evenly than in the oven, where there is a heat gradient from the rim to the center. We check for stiffness by squeezing the samples, examine the integrity at the surface with our fingers and cut them open to look if they are different in the center.

## 3.2. Structure reconstruction - Xray-tomography

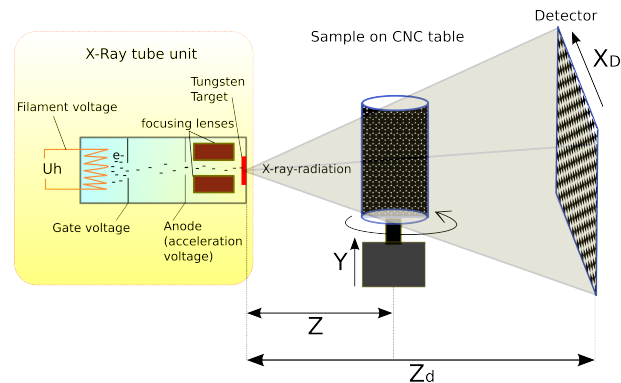


Figure 3.2.: Scheme of the Nanotom setup. The sample turns in small steps, while the detector takes radiograms of the scattered x-ray photons. [13]

In order to visualize the inner structure of the sediment samples we make use of the Computed Tomography system 'Nanotom' from the company Phoenix|x-ray. The Nanotom is an x-ray tomograph, which means that it uses x-rays to produce a three-dimensional picture of an object. In this case, x-rays are generated by decelerating free electrons on a tungsten target [13] (see **image 3.2**). The x-ray beam is then sent onto the sample, where it partly passes through and is partly absorbed or scattered. A detector records an absorption image, called radiogram. By turning the sample by 360 degrees in small steps and making a radiogram each step, the Nanotom constructs a volume data set or 3d picture, called tomogram. In our experiments the resolution of the tomograms ranges from 9 to  $10\mu\text{m}$  per voxel<sup>1</sup>. The samples used in this experiment are 2-3cm in height and 22.5mm in diameter. This is necessary as they have to be big enough to cover the detector from the x-ray beam. We produce tomograms of samples with different volume fractions of PDMS, filled either with air or water. The curing process of the sample is not important as it has no impact on the structure of a sample. Optionally, we dissolve the salts  $\text{ZnI}_2$  or  $\text{BrK}$  in the PDMS of some samples. The idea here is to generate a contrast between PDMS and glass beads. The goal of the tomography experiment is to find out if we will be able to examine cracks in a sample and how many different phases (glass beads, PDMS, medium, bacteria) we can distinguish in a tomogram.

---

<sup>1</sup>A voxel is the pixel of 3d images.

### 3.3. Elasticity measurement - The scale setup

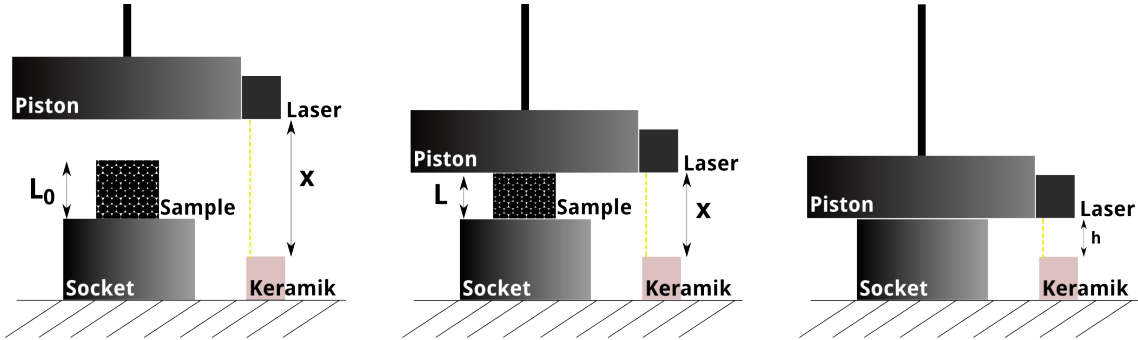


Figure 3.3.: Schemes of the scale setup defining  $x$ ,  $L$ ,  $L_0$  and  $h$ . The length  $x_0$  is the distance measured by the laser when piston and socket are the length  $L_0$  apart. The socket and keramik block rest on a scale, which measures the force on the sample.

We use the scale setup to determine the elasticity of our samples. The scale rests on a table, carrying the sample (see **image 3.3**). A translation stage moves a piston and a laser vertically at controllable speed. Both, weighing scale and laser, are read out digitally by a Labview program.<sup>2</sup> When the sample is compressed by the piston, we can measure the force on and the displacement of the sample. Following **section 2.3** we find that the stress  $\sigma$  is linked to the measured force and the strain  $\varepsilon$  to the compression  $\Delta L$  of the sample:

$$\sigma = \frac{F}{A} \quad (3.1)$$

$$\varepsilon = \frac{\Delta L}{L_0} \quad (3.2)$$

Using  $\Delta L = L_0 - L$  and the definitions of  $h$  and  $x$  made in **image 3.3**,  $\varepsilon$  can be re-written as

$$\varepsilon = \frac{L_0 - L}{L_0} = \left( \frac{x_0 - x}{x_0 - h} \right), \quad (3.3)$$

where  $x_0$  is the distance measured by the laser, when piston and socket are separated by the distance  $L_0$ . Before each run, the length  $h$  is measured with the laser. The data points consist of a measured mass  $m_{scale}$  and distance  $x$ . Because of surface

<sup>2</sup>Laser:  $\mu\epsilon$  optoNCDT 1402, Weighing scale: Denver Instruments TP-6101, Translations stage: Standa 8MT175.

### 3. Experimental setup

roughness the height  $L_0$  of the sample is more difficult to determine. Due to the roughness on the sample's surface, when the piston touches the sample the weighing scale measures a force, before there is a real compression of the sample's main body. So  $L_0$  is determined indirectly, when  $x_0$  is determined by a fit on the collected data points. This is a very accurate method with an error of 3-30 $\mu\text{m}$ .

We use a microscope to observe the bridges of PDMS, as they are too small to be seen by the naked eye. As we are interested in homogeneous samples we want to be sure we find well distributed capillary bridges in our samples. We conduct two different experiments:

- In the first experiment we examine segments of the surfaces of cured samples. Each segment is 14.5 x 22mm<sup>2</sup> in size. We count the number of bridges per bead in dependence of the amount of PDMS in a cured sample. If the PDMS is spread homogeneously we will find a large number of bridges of capillary shape (no trimers or pentamers, see **image A.1**) per bead.
- The second experiment is to find out how long we have to let a sample rest before beginning the curing process. Over two and a half hours we make a picture every ten minutes and measure the difference in bridge size. Again, we can only examine the surface of samples.

## 3.4. Microscopy

The microscope experiment lets us examine the same samples we use for qualitative studies, but for the bridge development observation experiment we also designed samples with a big surface area where we can more easily examine a flat surface (see **image 3.4**).

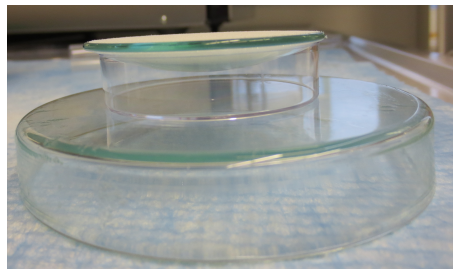


Figure 3.4.: Sample used in the microscope experiment. The flat and big surface allows good observation of capillary bridges.



## 4. Analysis

### 4.1. Qualitative properties of the sample

The immediate variations in sample properties found by testing the samples between the fingers are in stiffness and integrity of the material. While the samples kept at room temperature are uncured and soft, all other samples have become stiff and elastic. The first group also tends to low integrity, which means that beads on the surface rather stick to fingers and gloves than the sample. **Table 4.1** shows the results of the first run in a relative comparison. Over all, the samples with a volume fraction of 1 vol% are softer than the others, but there is no or a small difference between samples made with 2 or 3 vol% PDMS. When comparing cut surfaces to the original surfaces we cannot perceive a difference in either stiffness or integrity. Therefore the samples are quite homogeneous. Heating in a microwave oven makes the samples stiffer, but does not influence the integrity. This indicates that curing was more successful in these samples. As temperature control is not possible when using the microwave oven we abandon its use after the first experiment. The samples are already homogeneous without careful heating.

	curing temperature					
	relative stiffness			relative integrity		
	RT	50°C	50°C*	RT	50°C	50°C*
1 vol% PDMS	-	+	+	-	+	+
2 vol% PDMS	-	++	+++	-	++	++
3 vol% PDMS	-	+	+++	+	++	++

Table 4.1.: Relative stiffness/relative integrity of the qualitatively analysed samples of different PDMS volume fractions. RT stands for room temperature. \*: the sample was heated in a microwave oven before it was kept at 50°C. “Curing” time was 20h for all nine samples.

## 4.2. Structure reconstruction

A typical example of a reconstruction picture is shown on the left picture in **image A.2** (see appendix). It shows a horizontal cut through the tomogram. The individual beads can be seen and distinguished from the medium. On the other hand, we can not distinguish the PDMS from the beads. This is, because x-rays respond to different electron densities. Both, glass beads and PDMS consist of silicon based molecules and therefore look the same in the tomogram. We expected that adding the salts  $ZnI_2$  and  $BrK$  to the PDMS in solvable amounts would sufficiently increase its electron density and make it visible in the tomograms. However, the effect is too small to be seen in a tomogram. We can not really explain this, but we see no difference in the pictures.

So, at the moment the tomograms are good enough to make cracks visible, but not good enough to distinguish all four phases in the sample, namely beads, bridges, medium and organic tissue.

For further analysis we use the free program ImageJ. The right picture in **image A.2** shows a threshold picture. In our case it is a binary image where all pixels above a certain grey value are considered white and all pixels below black. Using such threshold sections through the tomogram we can determine the fraction of black area, representing the solid volume (glass beads and PDMS), in a sample. **Table 4.2** shows the results for such calculations for three samples. The samples were chosen, because of the good quality of the scans. The regions of interest were coaxial cylinders of nearly the full samples' height. About two millimeters were cut from the top and bottom, because of boundary conditions.

We see in all three scans the tendency to a higher solid content when the rim regions are included. This is due to a systematic error, when measuring center regions. Since the x-rays have to pass more matter, the center regions are depicted darker than the rim regions.

The determined fractions are close to the packing density of 57-58 vol% calculated in **chapter 2.1.1** for the glass beads. However, most values are smaller, even more so as there is an additional PDMS content of 1 vol% in scan 7 and 2 vol% in the other two.

Radius [px]	500	600	700	800	900
scan 7					
volume fraction [%]	54	55	56	57	58
error [%]	2	2	2	2	2
scan 8					
volume fraction [%]	54	54	55	56	57
error [%]	3	2	2	2	2
scan 10					
volume fraction [%]	54	56	58	60	64
error [%]	7	7	5	6	6

Table 4.2.: Volume fraction of solids in a sample as determined from the tomograms. The radius is that of a coaxial cylinder inside which the fraction was determined. The errors mainly result from the inaccuracy of the thresholding parameters, which we have to adjust manually.

## 4.3. Scale setup

### 4.3.1. Stress and strain calculation

With the obtained raw data we cannot describe the elastic behavior of the samples directly. We have to convert them into stress and strain first, which characterize elasticity. The stress  $\sigma$  can be calculated using

$$\sigma = \frac{F}{A} = \frac{m_{scale} \cdot g}{A}, \quad (4.1)$$

with  $g$  being gravitational acceleration. For the strain  $\varepsilon$  we need to determine the length  $x_0$ . We do this by plotting  $\sigma = \frac{F}{A}$  vs.  $x$  of one data set and then fitting the function

$$f(x) = C \cdot \left( \frac{x_0 - x}{x_0 - h} \right)^2 \quad (4.2)$$

to one leg of the data points. The two fit parameters are  $x_0$  and the third-order elasticity parameter  $C$  mentioned in **equation 2.4**. For the fit, its linear term is dropped, as  $E$  is zero. **Image 4.1** shows such a fit and the resulting fit parameters.

## 4. Analysis

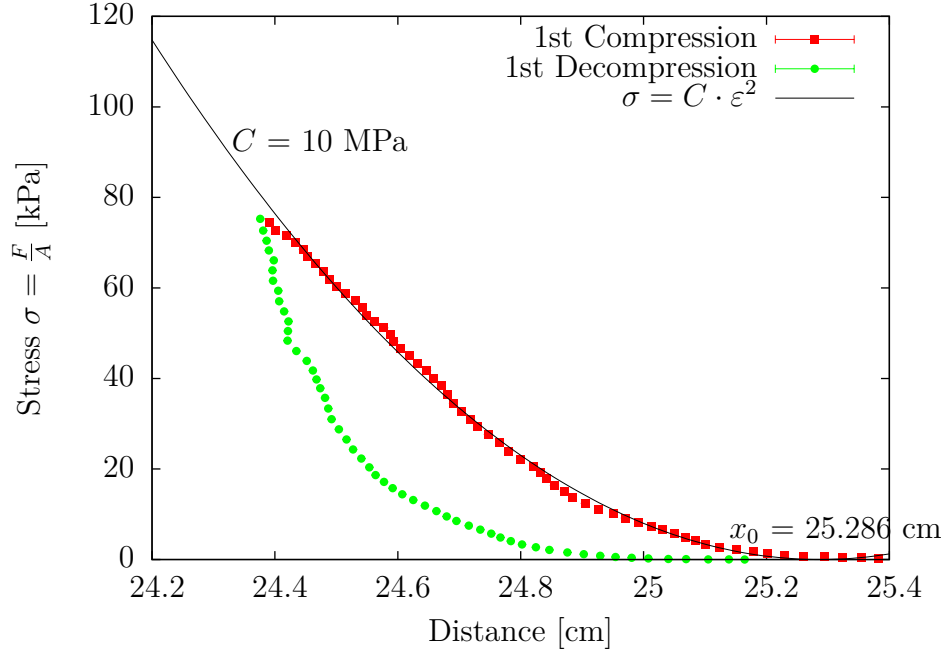


Figure 4.1.: The first compression-decompression cycle on a sample colored separately and a quadratic elasticity fit. The fitting function is shown in [equation 4.2](#).

### 4.3.2. Visualisation of data

Using this method we are now able to calculate  $x_0$  and then plot stress vs. strain curves for any sample. **Image 4.2** shows stress vs. strain for three compressions and decompressions in a row on the same sample. **Image A.3** shows the same plot, but with errorbars. The errorbars do not indicate individual errors of the data points, but rather errors of the whole curve.

We see that there is a hysteresis when decompression follows compression as both curves are not matching. After the first cycle, the other cycles follow the same hysteresis curve. This could be due to plastic deformation of the sample or the sample being viscoelastic. The plot shows, that the quadratic fit matches the curve well, so we really have a non-linear elastic behavior. This is also illustrated in **image 4.3**. Here stress and strain are plotted on a logarithmic scale. Except for a few data points below 2 kPa, the curve follows a straight line of slope 2. This confirms the accuracy of the quadratic law with disappearing linear term. The data points not on that straight line are caused by the rough surface of the sample. When the piston touches the beads on top of the sample, the weighing scale records a stress

before the main body of the sample is being compressed.

### 4.3.3. Behavior in deformation

In an elastic compression, for example compression of a spring, energy is stored in the compressed material. When the stress is released the material immediately restores its original shape. The fact that the decompression curve does not follow the compression curve shows that the deformation of the sample can not store all compression energy and is not purely elastic. There are two possible explanations for this phenomenon, namely viscoelastic and plastic deformation. Both of them occur here. Unlike an elastic material, a viscoelastic has a delayed response to stress. In plastic deformation no energy is stored and the material is permanently deformed. **Image 4.4** shows the viscoelastic behavior of a sample (2 vol% PDMS, base - agent ratio 10:1). After a short period where stress is held constant, the piston is held fixed in its position. Although strain is now held constant, stress begins to decrease. After about 1000 seconds the sample is released for 300 seconds, before the next run starts. The decrease in stress becomes smaller, but never stops. The

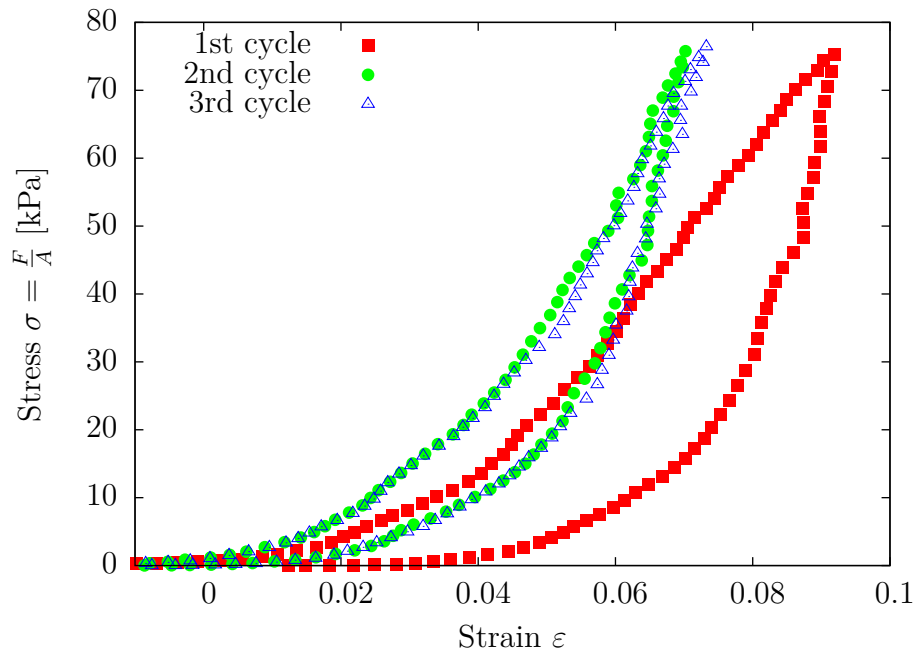


Figure 4.2.: Stress vs. Strain during a cycle of compression and decompression. There is a hysteresis between compression on the left leg and decompression. After the first cycle the following cycles are congruent.

#### 4. Analysis

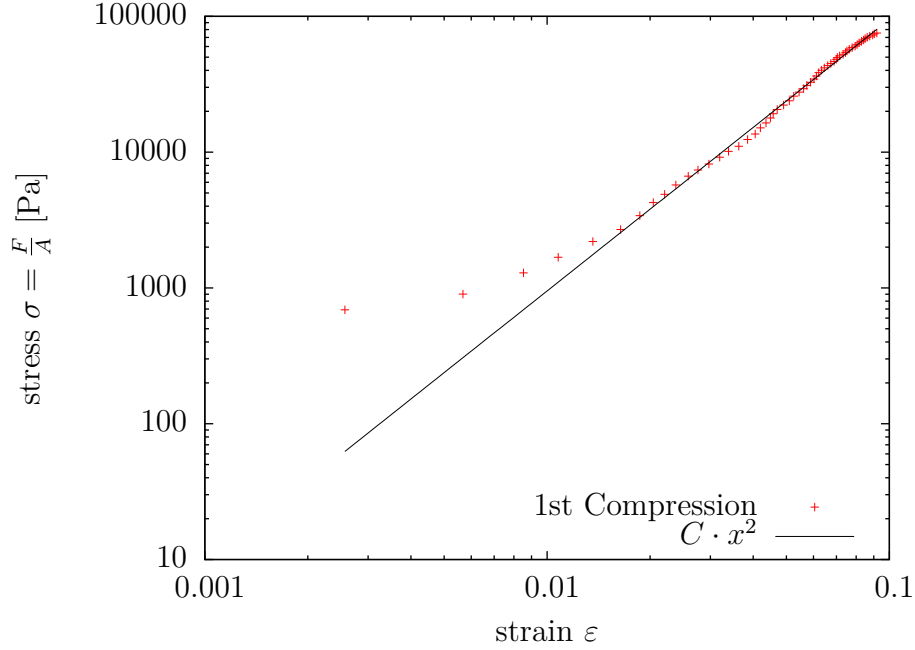


Figure 4.3.: Stress vs. strain in logarithmic scaling. Except for the data points below 2 kPa, the curve follows a straight line with slope 2, which shows that the relation really is that of a square law with no linear term. The data points leaving the straight line are due to the roughness of the sample. The contact with the piston occurs before it starts to compress the main body of the sample.

time-dependency of the stress (next to the strain-dependency) is characteristic for viscoelastic materials. It can be quantified as the slope of the straight stress-time curve in a double logarithmic plot. This is shown in **image 4.5**. The underlying relation between stress and time  $t$  is

$$\log(\sigma) = a \cdot \log(t) \Leftrightarrow \sigma = t^a, \quad (4.3)$$

where  $a$  is the slope of the straight line. As the sample is compressed to the same stress and therefore new strain each time, the  $a$  parameter is of different values for different runs.

We have already seen, that after the first compression-decompression cycle the curves of the following cycles are congruent. In **image A.4** we see four cycles measured on the same sample. The sample was let to rest for 23 hours between the second and third cycle. While second and fourth curves are very close, the sample could expand viscoelastically over night and the third cycle lays between the first

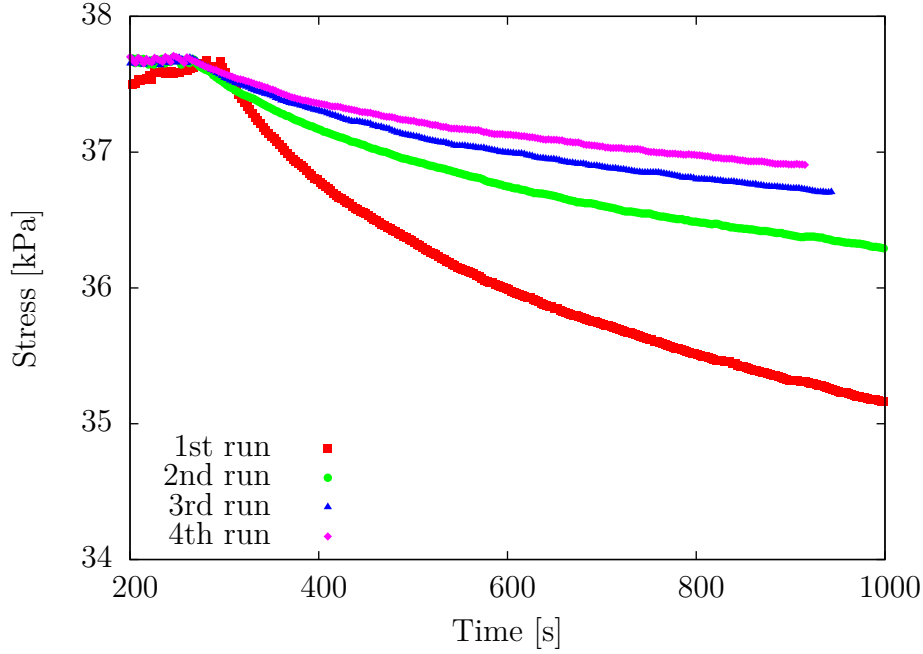


Figure 4.4.: Stress over time with constant strain. All four curves are of the same sample and follow each other with pauses of 300 seconds.

and the other cycles. When we look at the compression curves only (see **image A.5**), we see that the shape of the latter three curves look the same as they follow the quadratic law. In contrast to this, the curve of the first compression is not convex above a strain of 8%, but straight. This is a hint for plastic deformation. The other hint is that the sample could not expand to its original shape, as can be seen in the different position of the first and third compression curves. Of three more samples, two showed the same behavior at 8% strain and one at 6% strain. To compare the elastic behavior, we have plotted the decompression curves separately as shown in **image A.6**. Since it is physically justified that without stress there would be no strain, the four decompression curves were moved to end at the point (0:0). We see that the four curves follow the same path, which means that the elastic behavior does not change after the first compression.

#### 4.3.4. Curing time

One question we still have to answer is, how much time the PDMS in the sample needs for curing. In the bulk, PDMS cures at room temperature within a day, but we can not expect it to do the same when in small amounts as it is the case for capillary

#### 4. Analysis

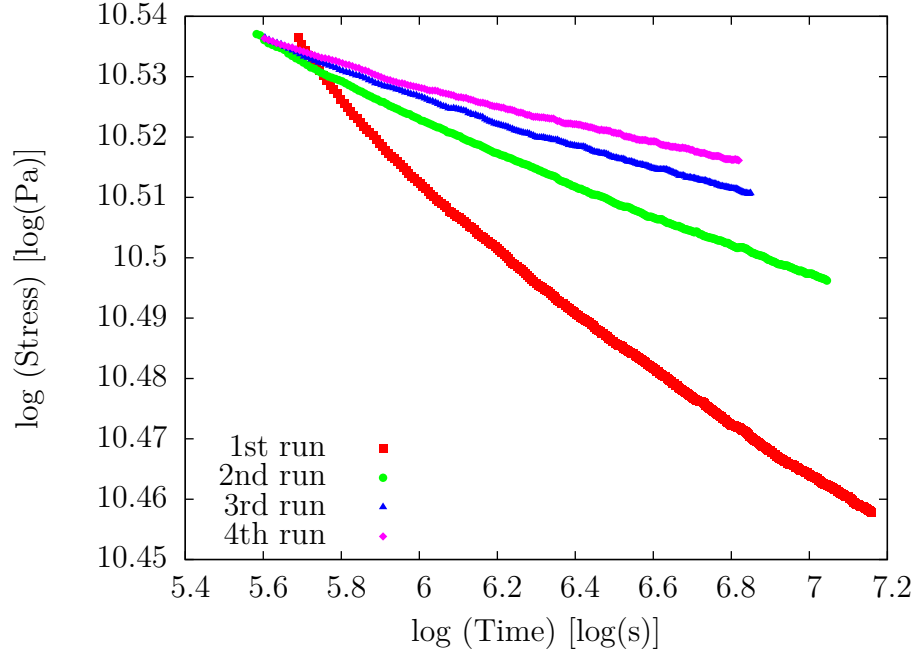


Figure 4.5.: Stress over time with constant strain in a double logarithmic plot. All four curves are of the same sample and follow each other with pauses of 300 seconds.

bridges in a wet granular material. So we record stress vs. strain curves for samples made of 2vol% PDMS (base:agent 10:1) cured at either room temperature, 50°C or 75°C and different times. The results are presented in **image 4.6**. The filled symbols represent curves of uncured samples. Those samples are not elastic and are being smashed by the piston. The curves marked with open triangles are completely cured. A longer curing time does neither move the curves significantly to the left ( $\rightarrow$  increased stiffness), nor does it significantly steepen the curves ( $\rightarrow$  increased elasticity). The curves marked with open circles show an intermediate state, where the sample is already cured, but not yet completely cured. The curve of the sample cured for 3h at 50°C shows that the sample cracked under the pressure of the piston at which point it started to be deformed plastically. The point where it cracked can be at ca. 6% strain, when the curve turns from convex to concave. We learn that the curing properties of PDMS in a sample are indeed different from the bulk. Curing at room temperature is not possible, while curing at temperatures higher than 50°C takes not as long. The transition stage lays between 1 and 3 hours at 50°C and 15 and 30 min at 75°C. The curing temperature has no effect on the sample's elasticity other than influencing the time required for curing.



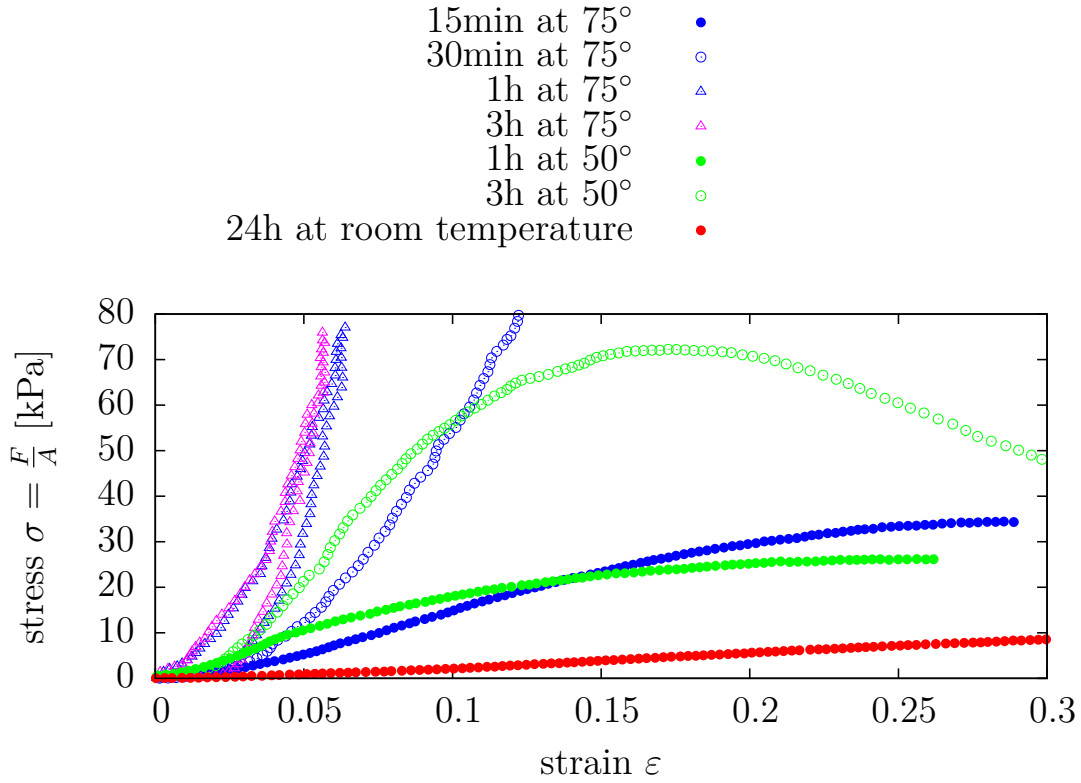


Figure 4.6.: Stress vs. strain for different parameters.

### 4.3.5. PDMS content

With the LANDAU modulus  $C$  we have a parameter to compare the elasticity of our samples. The greater  $C$  is, the greater is the stiffness of a sample. At first we try to influence  $C$  by varying the PDMS content in a sample. **Image 4.7** shows the values of  $C$  in dependence on the volume fraction of PDMS. This includes all completely cured samples ( $t = 15\text{h}$ ) at  $50^\circ\text{C}$ . Since the left has lots of widely spread data points, we calculate the weighted mean of all  $C$ -values around the same volume fraction and plot it vs. PDMS volume fraction. The data point marked in green is dropped for this calculation, because the sample already showed uncharacteristic behavior during the compression cycles. The plot is shown in **image 4.8**. The red bars mark the range of the original data points we calculated the weighted mean of. We see that we can influence, but not control the  $C$  parameter and therefore the elasticity of a sample by changing the volume fraction of PDMS. Though  $C$  is generally higher in samples with a volume fraction of 2 vol% than in 1vol% samples, the possible range of  $C$  for 2 vol% samples is higher than the difference between the

#### 4. Analysis

mean values of both groups. In other words, the difference between the 2% samples is greater than the difference between samples of 1 and 2%.

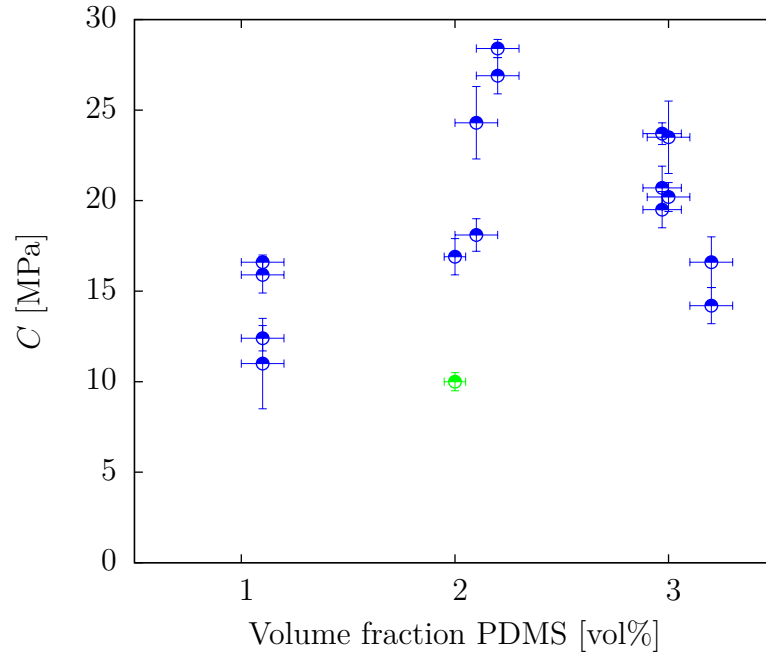


Figure 4.7.: The parameter  $C$  in dependence on the volume fraction of PDMS. All samples are completely cured (15h at  $50^\circ$ ). The green data point is considered faulty and is dropped for further analysis.

#### 4.3.6. PDMS composition

Another way to influence the elasticity or stiffness of the sample is to vary the composition of PDMS used in a sample. **Image 4.9** shows  $C$  in dependence of the mass fraction of curing agent in the PDMS. In this experiment PDMS volume fraction was at 2% and all samples were completely cured. There seem to be two curves for the two different curing temperatures. On the other hand, it is shown that by decreasing curing agent content  $C$  can be lowered in a wide range from 25-5MPa. For comparison, the cured samples in **image 4.6** are at  $C = 20.1$ (purple triangles),  $C = 16.1$ (blue triangles) and  $C = 5.5$ (blue circles).

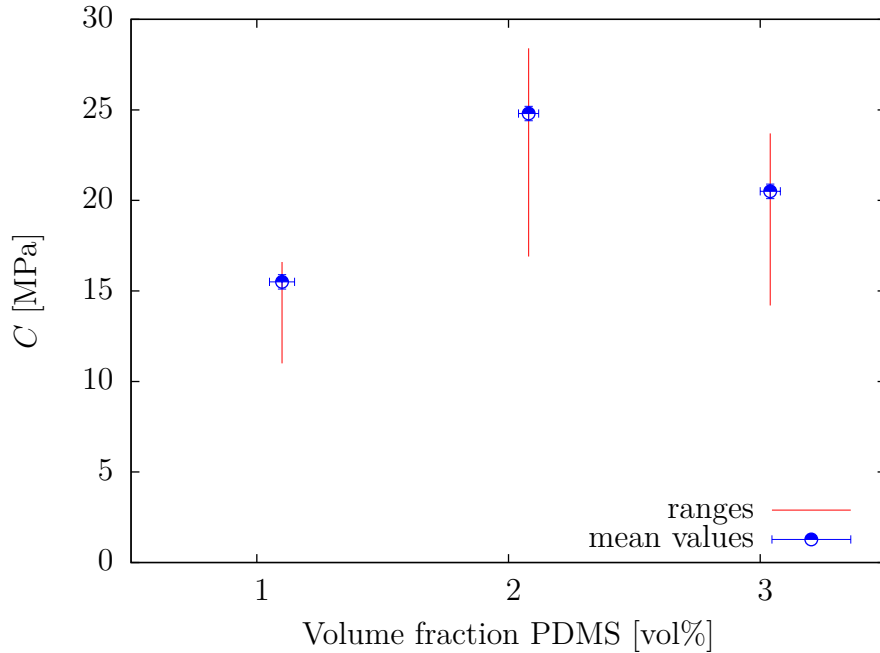


Figure 4.8.: Weighted mean of the data points in **image 4.7** around one volume fraction. The red bars indicate the range of the original data points. The point at (2,10) was dropped.  $C$  can be varied from 15-25 MPa, but the control through changing the volume fraction of PDMS is not high.

## 4.4. Microscopy

We determine the average number of cured bridges per bead (bpb) by counting all beads and all bridges on two or three surface segments (size:  $14.5 \times 22\text{mm}^2$ ) of 18 different samples. The number ranges from  $(2.6 \pm 0.1)$  bpb at 1 vol% PDMS, over  $(3.1 \pm 0.1)$  bpb for 2 vol% to  $(3.2 \pm 0.1)$  bpb at 3 vol%. The bridge sizes range from  $30\text{-}130\mu\text{m}$ . Next to simple bridges connecting two beads, we find more complex ones in the samples with higher PDMS content, forming trimers and pentamers (see **image A.7**).

The long-term observation of capillary bridges shows that most bridges increase in size, but some decrease. Not all bridges are clearly saturated after two and a half hours. **Images 4.10 to 4.13** show the development of bridge length  $L$  over the time of 150 minutes. **Image A.8** shows the observed bridges at time  $t=0$  minutes. The time between data points is ten minutes, PDMS content is at 2 vol%, base - agent ratio is 10:1. The errors are due to an inaccuracy of  $2\mu\text{m}$  when measuring bridge length. Most bridges grow by  $10 \pm 5\%$  over 150 minutes, but some shrink (bridges 4,

#### 4. Analysis

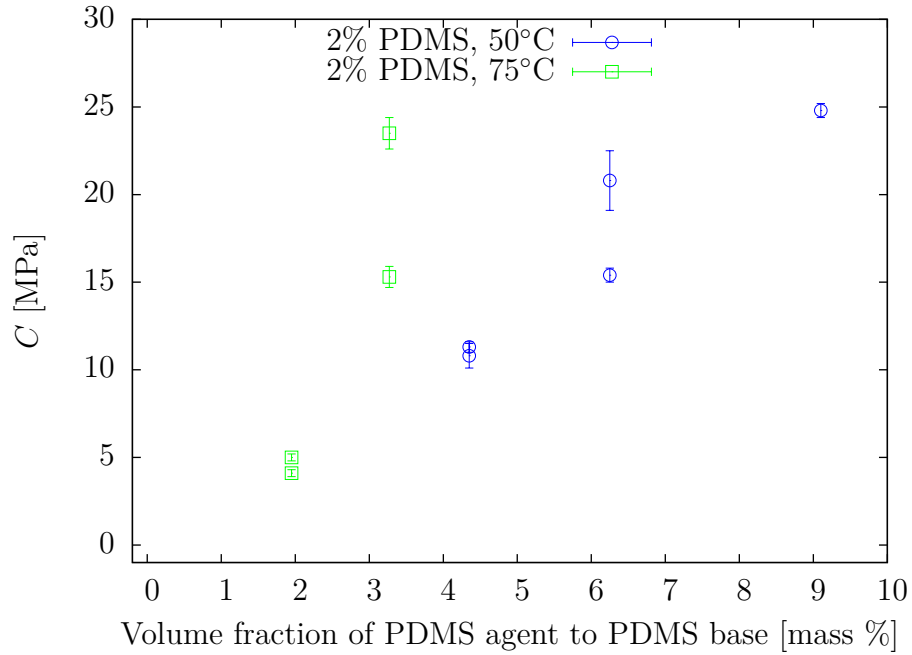


Figure 4.9.: The parameter  $C$  in dependence on the mass fraction of curing agent in the PDMS. All samples were completely cured (curing time: 15h).  $C$  can be varied from 5-25 MPa by varying the fraction of curing agent in the PDMS.

7, 12). Since the PDMS distribution has to equilibrate this is not surprising. Also, after 100 minutes most bridges show no or only small changes until the end. An exception to this are bridges 4, 7, and 11 which show activity in the last 10 or 20 minutes. The jumps which sometimes occur, for example bridge 14 at 90 minutes can be due to faulty measurements. Something interesting happened to bridge 7. Between 50 and 60 minutes it joined with two other bridges to form a trimer. We learn that after 150 minutes the PDMS distribution is equilibrated or at least close to being equilibrated. So we can start curing the samples after 2.5 hours of resting time.

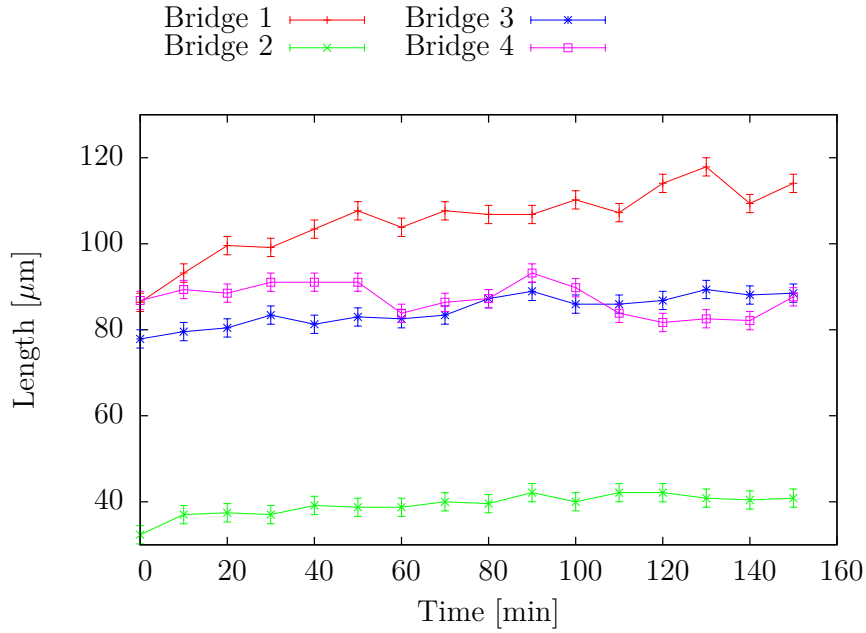


Figure 4.10.: Development of bridges 1-4. The data points are ten minutes apart. The errors result from an inaccuracy of  $2\mu\text{m}$  when measuring bridge length.

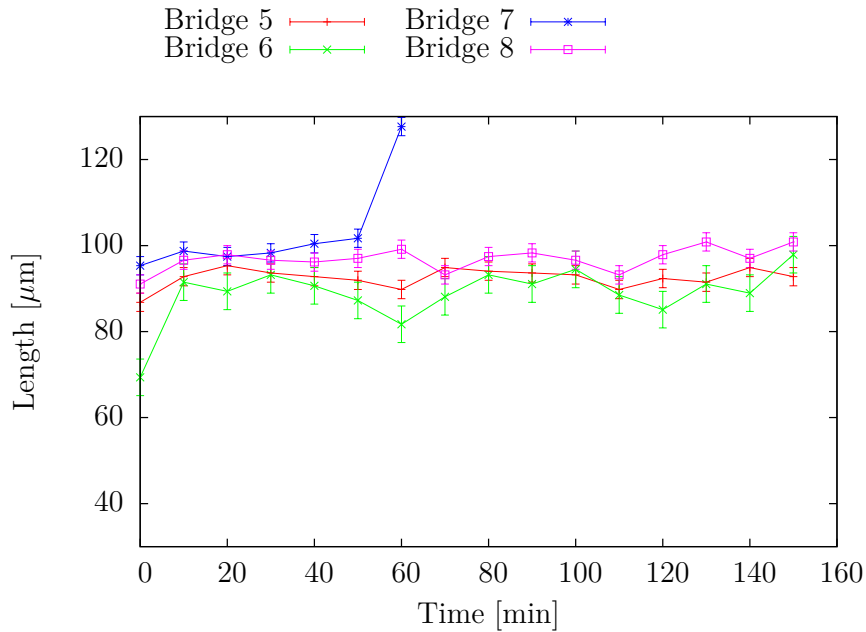


Figure 4.11.: Development of bridges 5-8. The data points are ten minutes apart. The errors result from an inaccuracy of  $2\mu\text{m}$  when measuring bridge length.

#### 4. Analysis

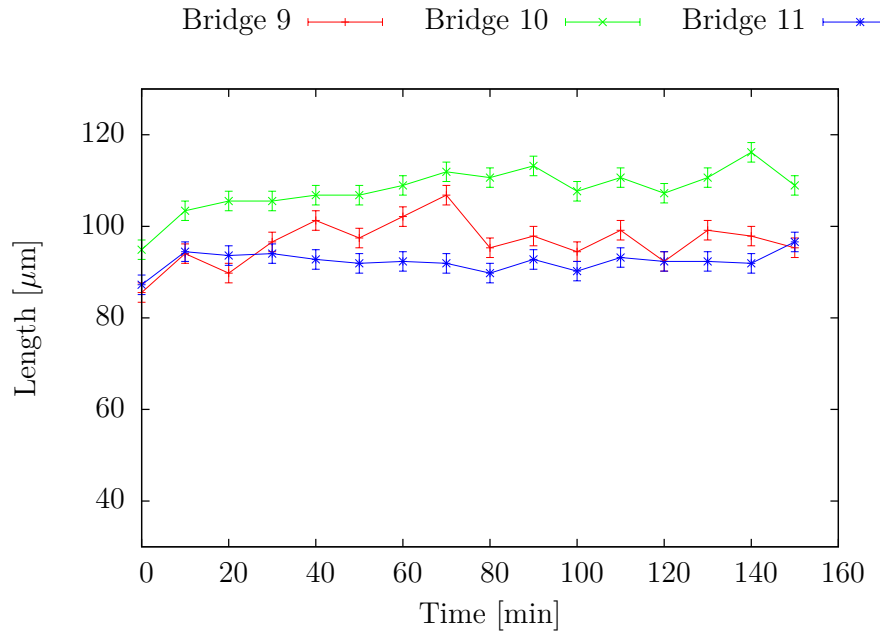


Figure 4.12.: Development of bridges 9-11. The data points are ten minutes apart. The errors result from an inaccuracy of  $2\mu\text{m}$  when measuring bridge length.

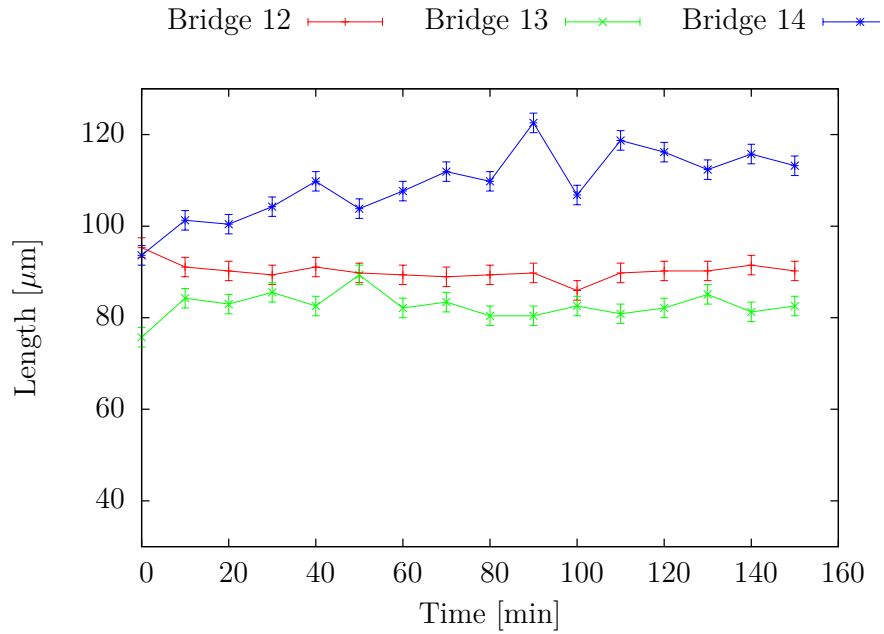


Figure 4.13.: Development of bridges 12-14. The data points are ten minutes apart. The errors result from an inaccuracy of  $2\mu\text{m}$  when measuring bridge length.

## 5. Discussion

The results of the different experimental setups add up to a good understanding of the properties and behavior of the samples. We have established a protocol for sample preparation and successfully conducted a row of experiments varying all parameters of the preparation process. The elastic model we applied was found to describe our samples very well. We now have a good idea which are the key parameters to elasticity control.

### 5.1. Qualitative properties of the granulate

The samples have rigid structures and can easily be produced in packages of up to 9 samples. Curing at room temperature is not an option for the PDMS bridges.

### 5.2. Structure reconstruction

We find that with the nanotom we are able to visualize the inner structure of the samples, which is important to find cracks produced by micro-organisms. We are not yet able to distinguish PDMS from glass beads as salts dissolve in PDMS in too small amounts.

When examinig scans to determine the solid content fraction of the sample we encounter two problems. First it is difficult to decide at which grey value to apply the treshold when separating solids from liquids. Second, the same grey values are not caused from the same electron density when comparing central beads with those close to the rim. This makes averages across the entire sample inaccurate. A way to improve results would be to focus only on one region when choosing the treshold parameter and then measure solid contents only in that region. One could also calibrate the grey values with beads in the different distances to the center.

### 5.3. Scale

We have found that in our experiment, with stresses up to 80 kPa and strains up to 10%, stress is a quadratic function in strain.

$$\sigma(\varepsilon) = C \cdot \varepsilon^2 \quad (5.1)$$

This is consistent with an elasticity model of third order in energy. The parameter  $C$  lets us compare the stiffness of samples. Therefore  $C$  is the tool for finding the key parameters to control sample elasticity and through this adjust necessary forces for cracking the samples. We have found the mass fraction of curing agent in PDMS and curing time to be key parameters for elasticity control. Although the PDMS content does have an influence on the samples' stiffness, the range of stiffness at one PDMS volume fraction is too big to control the stiffness of a certain sample. At room temperature capillary bridges of PDMS do not cure. The lowest curing temperature we know of is 50°C. Apart from that, curing temperature influences curing time in how long a sample needs to be cured, but not in elasticity control range due to curing time. We identified PDMS base - curing agent mass ratio as key parameter, but need more data on this parameter. If the effect on elasticity really is dependent on temperature, it might be that the curing agent mass ratio has an impact on what curing time is needed.

We have confirmed that the samples deform mainly viscoelastically, but also plastically above a certain strain (8%). This is a good property as we want microorganisms to produce cracks on the inside.

### 5.4. Microscopy

The number of bridges per bead counted on surfaces is consistent with values we could expect. In the bulk, a number of at least six bpb is to be expected[1], as six contact points can stabilize a bead in the three dimensions of space. This is also found experimentally as shown in **image A.9**[2]. The number of bridges per beads can only be reduced by combining them to bigger objects, like trimers. For beads on the surface the contact points on the top are saved. Since we are limited to examination of the surface at least one more contact point will be hidden from us. Our findings of 3-4 bpb are therefore consistent with the minimal number of contact points needed to stabilize a bead on the sample's surface.



The bridge development experiment shows that for a good equilibration we need to wait 3 hours rather than 2 as we did with our samples. This changes our protocol for sample preparation by increasing resting time by 1 hour. Through the good distribution of PDMS we obtain homogeneous samples.



## 6. Concluding remarks

Now that we have an idea in what range we can control the samples' elasticity, we can continue and add bacteria to the sample. There is already an existing setup for this [14]. There are also some new ideas how the results presented in this thesis could be improved or supported. To support curing agent mass fraction as a key parameter to elasticity control more data should be collected. This need not necessarily be with further measurements using the scale setup. A better way to measure elasticity of a material is to measure its *tensile strength* [1]. We used the scale setup, because it was available and measuring automatically. In compressing the sample we have bead to bead collisions or beads evading to the side and other undesired effects, which are difficult to account for in analysis. In a tensile strength experiment we would pull on the sample and mostly measure elastic components of the PDMS bridges. For example, the sample could be suspended vertically with a weight attached to the bottom. In this scenario, stress would be force divided by the sample's cross-sectional area and strain the normalized increase in length.

As mentioned before, we want to distinguish four phases in the x-ray tomograms: beads, bridges, medium and bacterial tissue. As the pure salts do not dissolve in PDMS in sufficient amounts, a promising idea is to mark PDMS-dissolvable molecules with Br-groups. To visualize the bacteria we can use that *e. coli* are gram negativ organisms. They can be marked with iod-based gram dye and will thus be visible in a tomogram.

In the microscopy experiments we were able to just explore the surfaces of samples. Here the idea is to submerge the sample in a liquid with the same refractive index as our glass beads [1]. Then the PDMS bridges could be analysed below the surface.



# A. Appendix


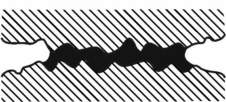
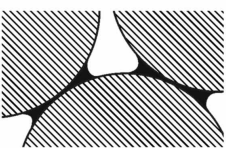
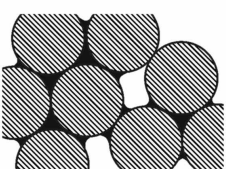
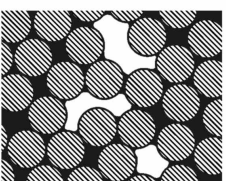
wetness regime		morphology	liquid content
humidity	asperities		$W = 0.0$ to $0.026$
	roughness		
pendular			
funicular			
			← $W^*$
		clusters	0.026 to 0.08
		bicontinuous	0.08 to 0.28
bubbles			0.28 to saturation

Figure A.1.: Regimes of wetness in granular media. The pendular regime is characterized by spherical grains and a liquid content between 0.0 and 2.8%. [1]

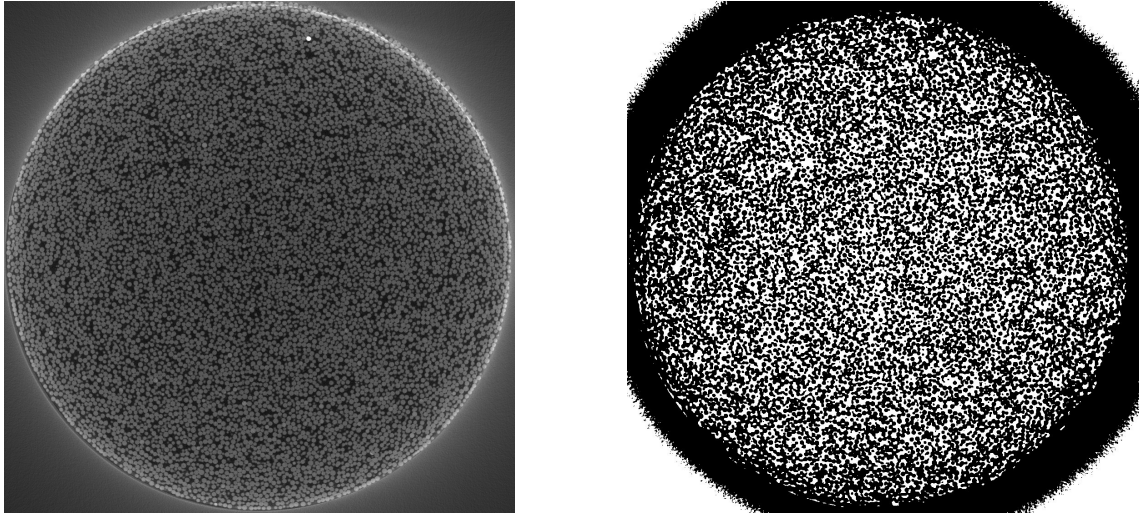


Figure A.2.: *Left:* Horizontal section through a nanotom reconstruction file (= tomogram). The individual beads are well distinguishable from the medium, which is in this case water. The bright bead close to the rim at one o'clock has probably incorporated some salt during production. *Right:* Binary conversion of the picture on the left. The threshold parameter is chosen to make glass beads and PDMS appear in black and the surrounding medium in white. The gray area outside the tube has become one black and one white region.

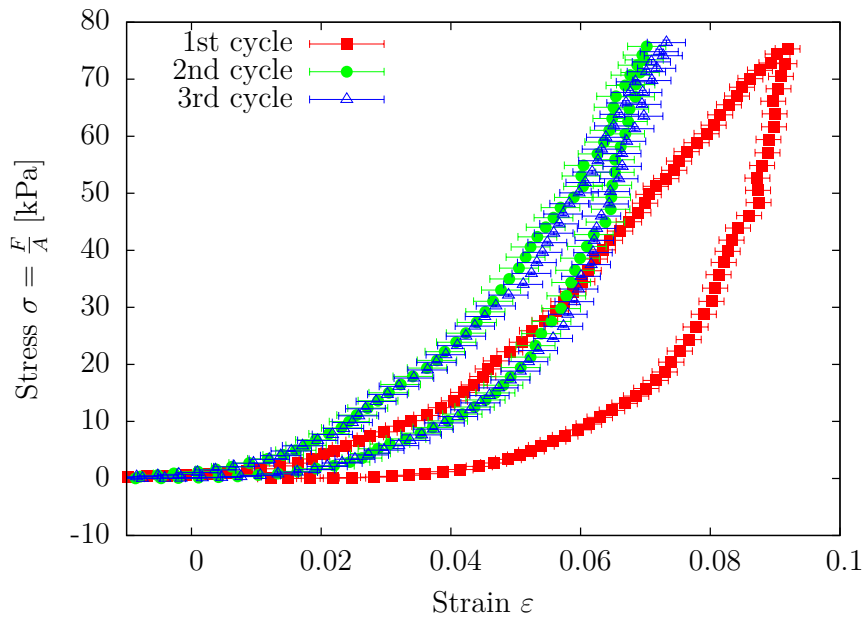


Figure A.3.: Stress vs. Strain during a cycle of compression and decompression with errorbars . The strain errors do not depict the errors in measuring the strain, but in the position of the curve.

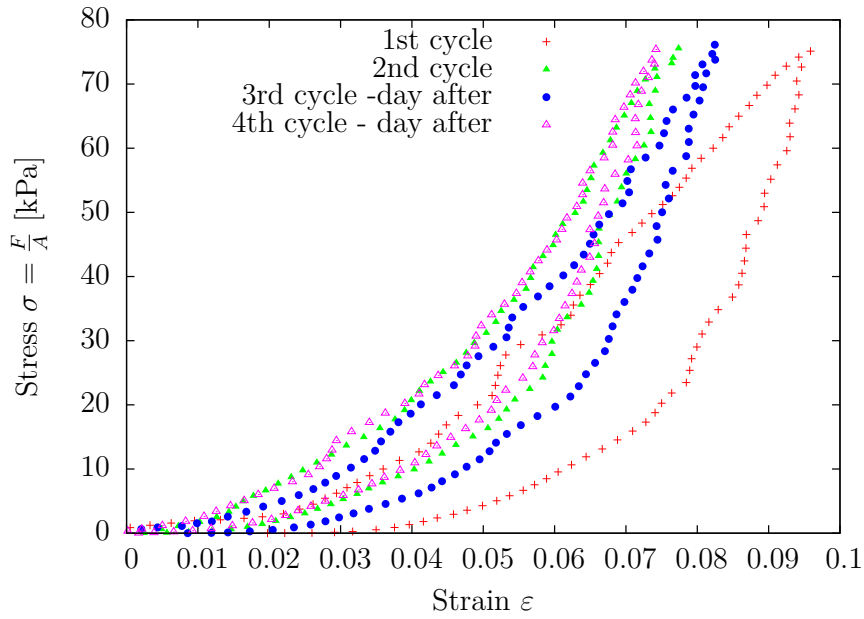


Figure A.4.: Four compression-decompression cycles of the same sample. Between the second and third run the sample was left to rest for 23 hours. While the second and fourth curve are congruent, the third curve has moved closer to the first one.

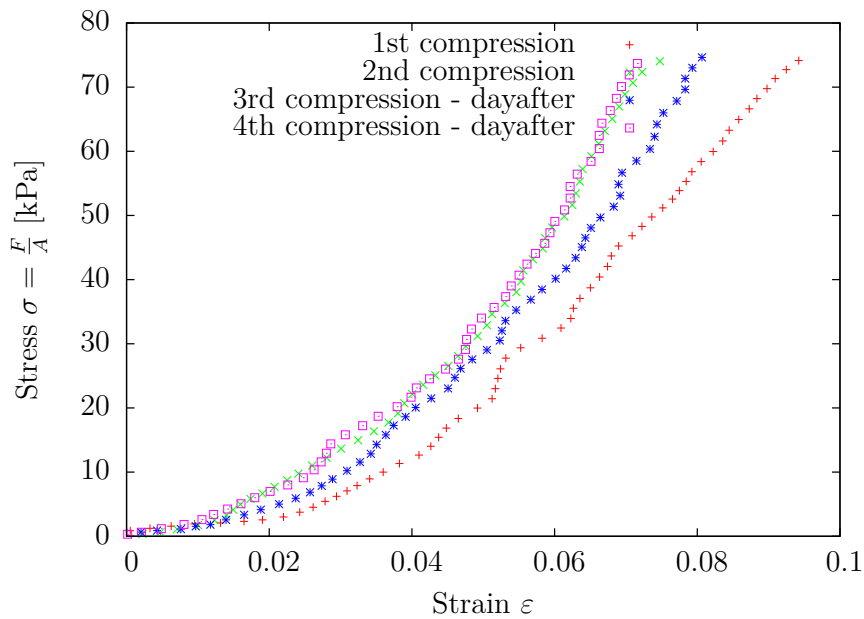


Figure A.5.: The compression curves of **image A.4**. The first compression seems to have deformed the sample plastically as it has a different shape than the other three curves.

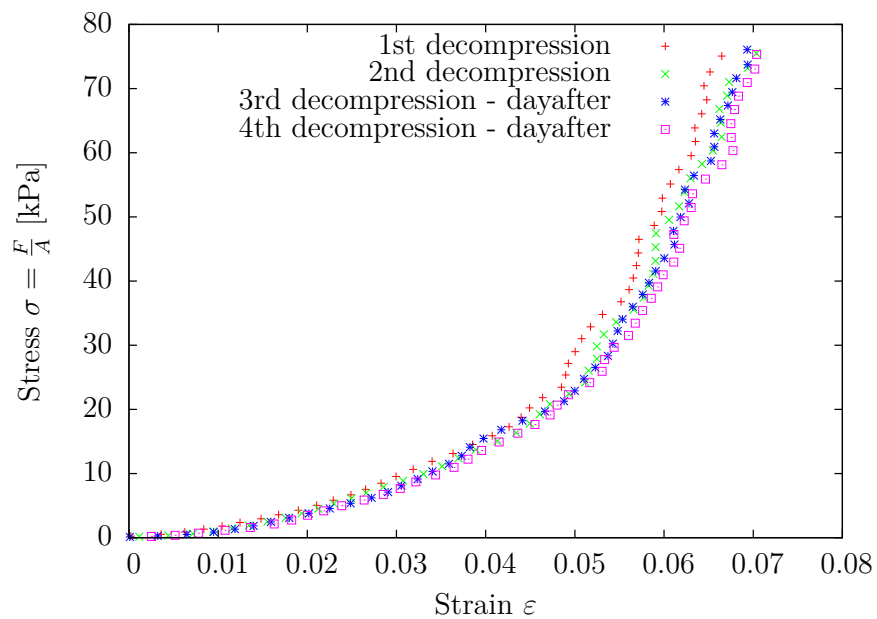


Figure A.6.: The decompression curves of **image A.4** shifted to meet at zero stress, zero strain. The curves are on top of each other, which shows that the elastic behavior is the same in all four measurements.



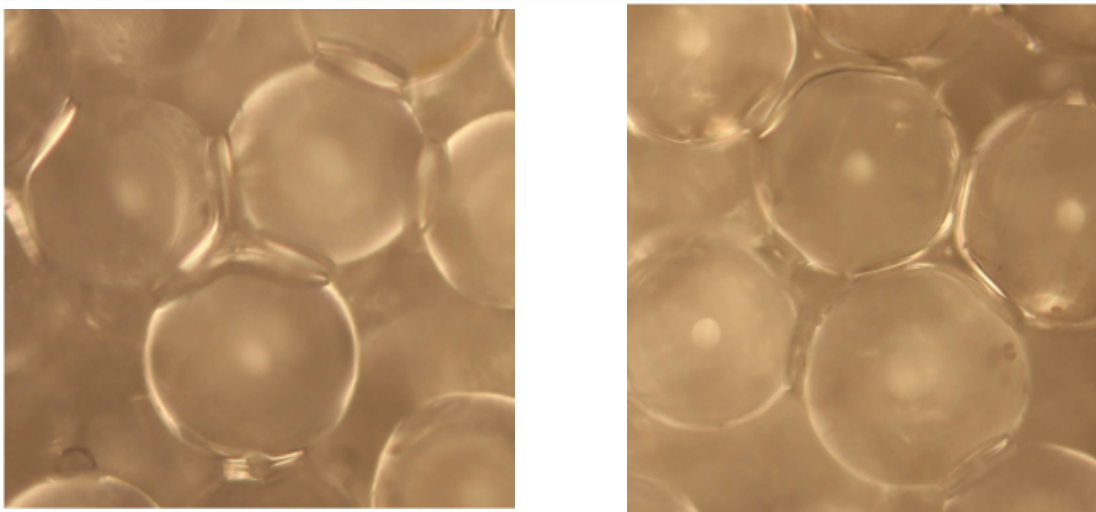
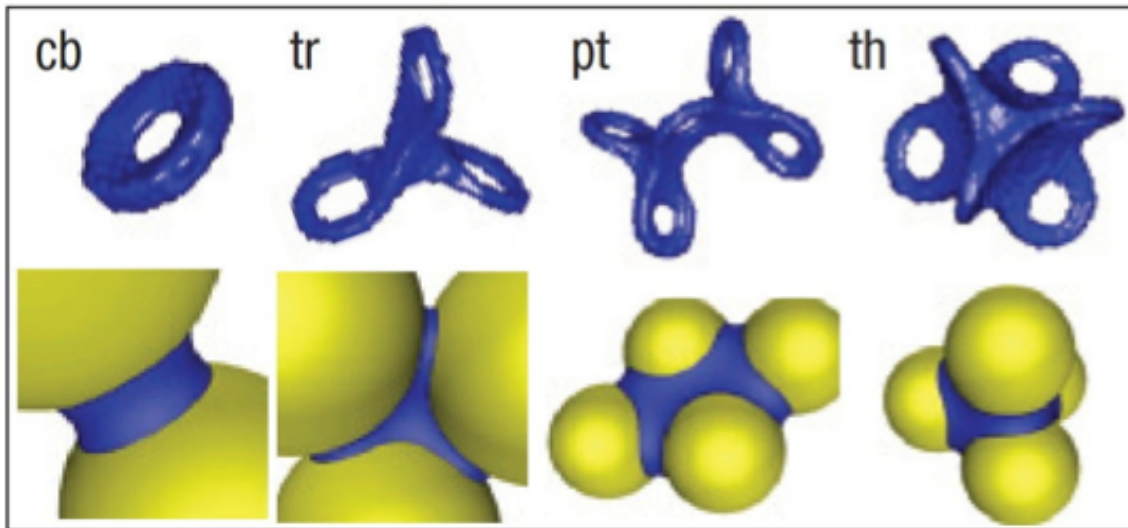


Figure A.7.: Examples for a trimer (left) and pentamer (right). 'cb': capillary bridge, 'tr': trimer, 'pt': pentamer [2]

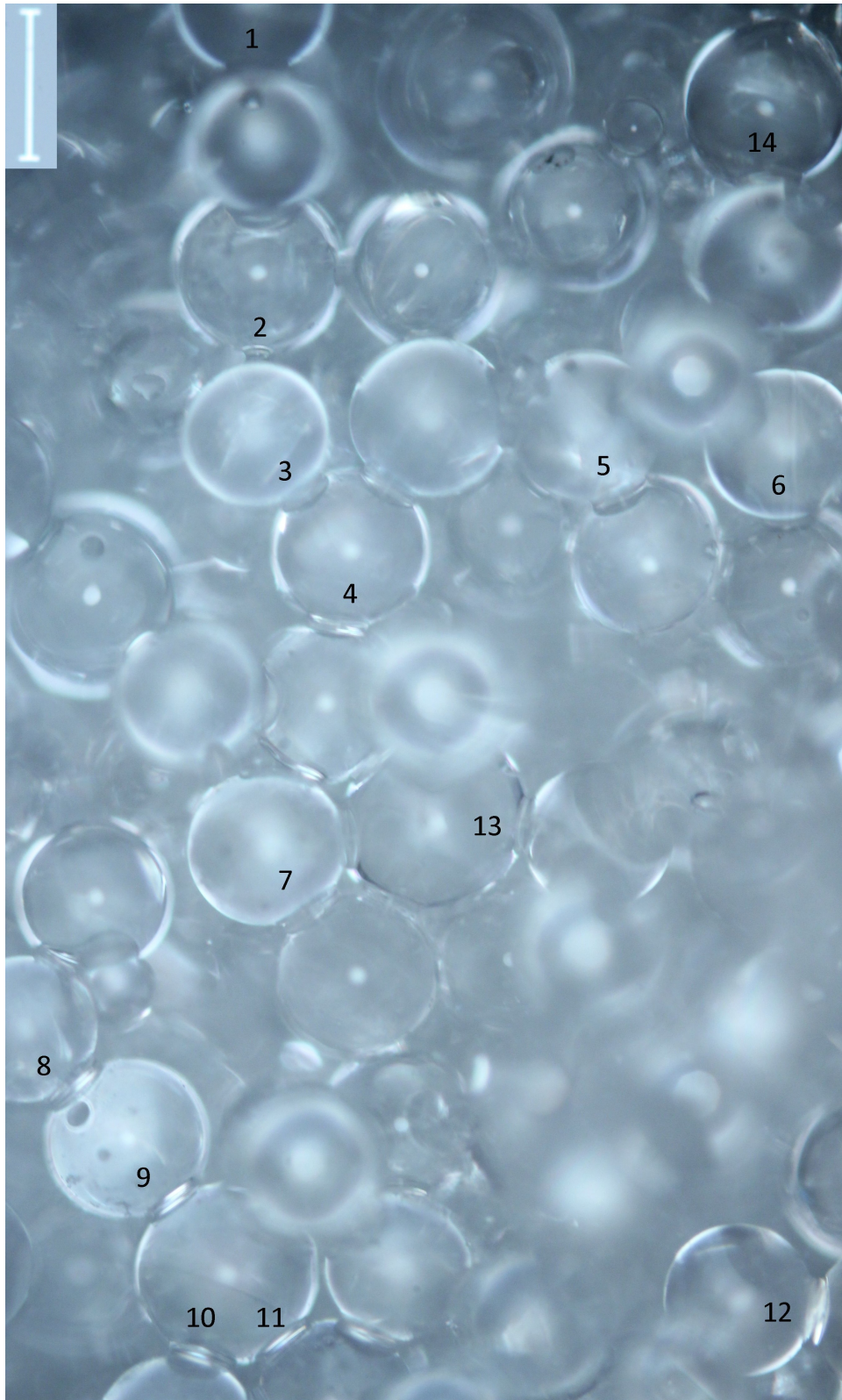


Figure A.8.: Sample segment with observed bridges 1-14. The bar shows the length of  $200\mu\text{m}$ .

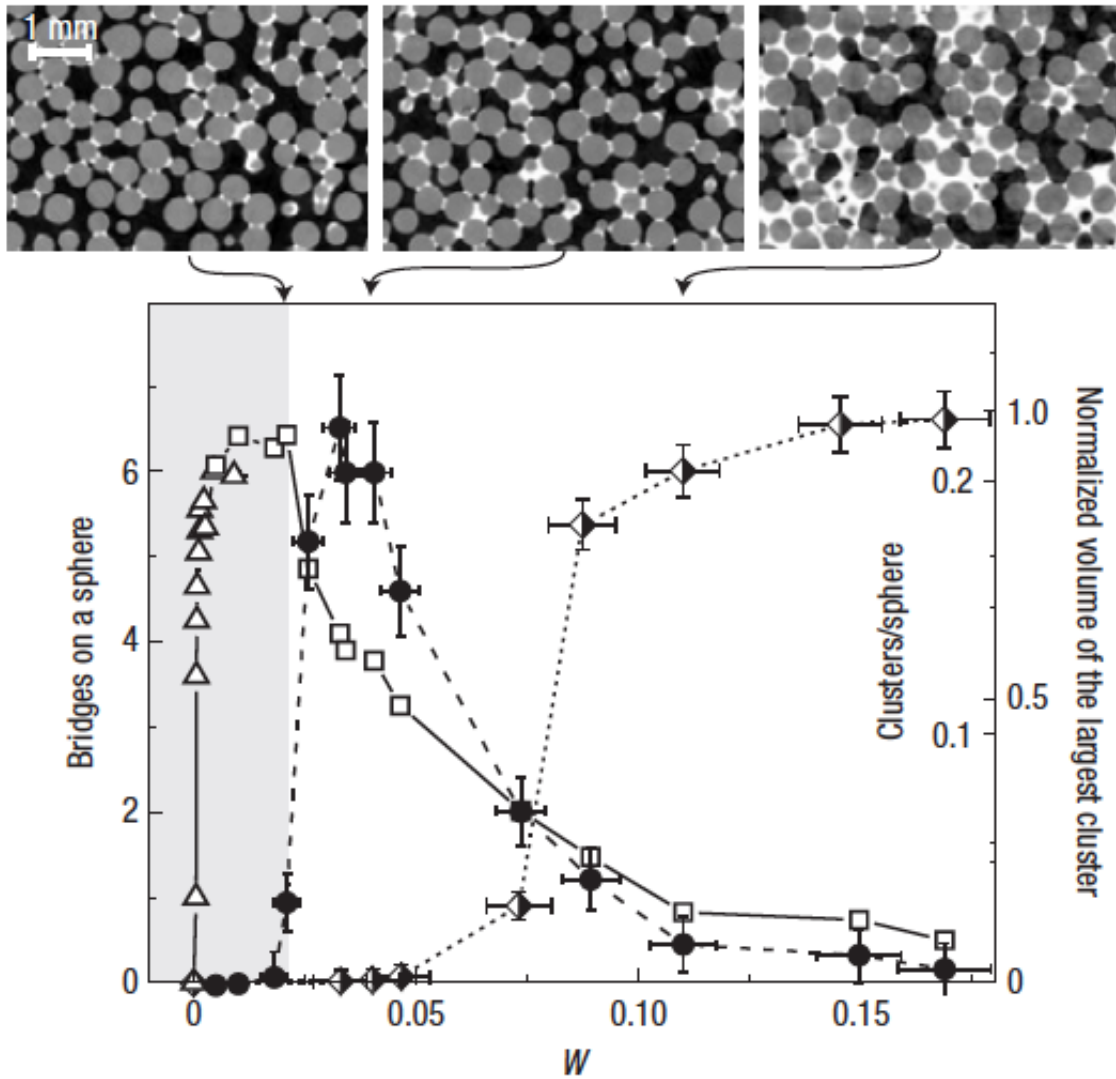


Figure A.9.: Main panel: frequencies of liquid objects at different water contents. Left axis: average number of bridges per bead (open symbols), right axis: average size of clusters per bead (filled symbols) and normalized volume of the largest cluster (half open symbol). Images on top: sections through tomograms of wet granular piles at  $W=0.02$ ,  $0.04$  and  $0.11$ . They refer to the pendular, funicular and bubbles regime (see image A.1). [2]



# Bibliography

- [1] HERMINGHAUS, STEPHAN: *Wet Granular Matter: A Truly Complex Fluid*  
World Scientific Publishing, 2013
- [2] SCHEEL, M. ET AL.: *Morphological clues to wet granular pile stability*  
Nature Materials, 7:189-193, 2008
- [3] ALLSOPP, DENNIS, SEAL, KENNETH J., AND CHRISTINE C. GAZLARDE:  
*Introduction to Biodeterioration*  
Cambridge University Press, USA, 2004
- [4] HUECK-VAN DER PLAS, E.H.: *The biodeterioration of materials as part of  
hylobiology*  
Mater. Organismen, 1:5-34, 1965
- [5] WARSCHEID, TH., AND J. BRAAMS: *Biodeterioration of stone: a review*  
Int. Biodeterioration and Biodegradation, Elsevier, 46:343-368, 2000
- [6] [http://education.mrsec.wisc.edu/nanolab/PDMS\\_fluidics/index.html](http://education.mrsec.wisc.edu/nanolab/PDMS_fluidics/index.html)
- [7] [http://www.infobarrel.com/Media/Heap\\_of\\_Sand](http://www.infobarrel.com/Media/Heap_of_Sand)
- [8] DOW CORNING EUROPE S.A.: *SYLGARD(R) 184 SILICONE ELAS-  
TOMER KIT BASE information*  
Version 2.0, sdseu@dowcorning.com, 09/19/2012
- [9] DOW CORNING EUROPE S.A.: *SYLGARD(R) 184 SILICONE ELAS-  
TOMER KIT CURING AGENT information*  
Version 2.1, sdseu@dowcorning.com, 08/01/2011
- [10] [http://en.wikipedia.org/wiki/escherichia\\_coli](http://en.wikipedia.org/wiki/escherichia_coli)
- [11] LUCAS GOEHRING: *Drying and cracking mechanisms in a starch slurry*  
BP Institute for Multiphase Flow, Cambridge, UK, 2009

## Bibliography

- [12] LANDAU, L. D. AND E. M. LIFSHITZ: *Theory of elasticity*  
Pergamon Press, Bristol, UK, 2nd Edition, 1970
- [13] MAX NEUDECKER: *PhD thesis*  
Max-Planck-Institut für Dynamik und Selbstorganisation, 2014
- [14] ALEXANDER SCHMEINK: *Biodeterioration of stone*  
Bachelor internship, Max-Planck-Institut für Dynamik und Selbstorganisation, 2014
- [15] OSTROVSKY, L. A. AND P. A. JOHNSON:  
Rivista del Nuovo Cimento 24, 1, 2001
- [16] ORTEGA-CALVO, J.J., M.HERNANDEZ-MARINE, AND C. SAIZ-JIMENEZ:  
*Biodeterioration of building Materials by Cyanobacteria and Algae*  
Int. Biodeterioration, Elsevier, 28:165-185, 1991
- [17] ORTEGA-CALVO, J.J., X. ARIÑO, M.HERNANDEZ-MARINE, AND C. SAIZ-JIMENEZ: *Factors affecting the weathering and colonization of monuments by phototrophic microorganisms*  
The Science of the Total Environment, Elsevier, 167:329-341, 1995
- [18] GOMEZ-ALARCON, G., M. MUÑOZ, X. ARIÑO, AND J.J. ORTEGA-CALVO: *Microbial communities in weathered sandstones: the case of Carrascosa del Campo church, Spain*  
The Science of the Total Environment, Elsevier, 167:249-254, 1995
- [19] NEUDECKER, MAX: *Master-FP: Versuch Röntgentomographie - Versuchsanleitung*  
Max-Planck-Institut für Dynamik und Selbstorganisation, 2010
- [20] <http://en.inotek.net/microspherethick-walled>
- [21] <http://www.verder.de/pumpen/schlauchpumpen/function-principles/>
- [22] <http://de.wikipedia.org/wiki/Bremsstrahlung>

# Danksagung

For help with this work, may it be guidance, input, answering questions or helping with measurements I say “Thank You” to

Arnaud Hemmerle, Markus Benderoth, Markus Richter, Wolf Keiderling, Julie Muri-son, Max Neudecker, David Meulemeester, Lucas Goehring and Stephan Herminghaus.

**Erklärung** nach §13(8) der Prüfungsordnung für den Bachelor-Studiengang Physik und den Master-Studiengang Physik an der Universität Göttingen:

Hiermit erkläre ich, dass ich diese Abschlussarbeit selbständig verfasst habe, keine anderen als die angegebenen Quellen und Hilfsmittel benutzt habe und alle Stellen, die wörtlich oder sinngemäß aus veröffentlichten Schriften entnommen wurden, als solche kenntlich gemacht habe.

Darüberhinaus erkläre ich, dass diese Abschlussarbeit nicht, auch nicht auszugsweise, im Rahmen einer nichtbestanden Prüfung an dieser oder einer anderen Hochschule eingereicht wurde.

Göttingen, den 28. Januar 2014

(Alexander Heinrich Schmeink)